BMC Cancer

RESEARCH

Open Access

Acetylation of PGK1 at lysine 323 promotes glycolysis, cell proliferation, and metastasis in luminal A breast cancer cells

Xiuli Gao[1], Ting Pan[2], Yu Gao[3], Wenbin Zhu[1], Likun Liu[1], Wenbo Duan[2], Cuicui Han[4], Bo Feng[5], Wenjing Yan[4], Qiuhang Song[6], Yunlong Liu[7*] and Liling Yue[1*]

Abstract

Background In prior research employing iTRAQ (Isobaric Tags for Relative and Absolute Quantitation) technology, we identified a range of proteins in breast cancer tissues exhibiting high levels of acetylation. Despite this advancement, the specific functions and implications of these acetylated proteins in the context of cancer biology have yet to be elucidated. This study aims to systematically investigate the functional roles of these acetylated proteins with the objective of identifying potential therapeutic targets within breast cancer pathophysiology.

Methods Acetylated targets were identified through bioinformatics, with their expression and acetylation subsequently confirmed. Proteomic analysis and validation studies identified potential acetyltransferases and deacetylases. We evaluated metabolic functions via assays for catalytic activity, glucose consumption, ATP levels, and lactate production. Cell proliferation and metastasis were assessed through viability, cycle analysis, clonogenic assays, PCNA uptake, wound healing, Transwell assays, and MMP/EMT marker detection.

Results Acetylated proteins in breast cancer were primarily involved in metabolism, significantly impacting glycolysis and the tricarboxylic acid cycle. Notably, PGK1 showed the highest acetylation at lysine 323 and exhibited increased expression and acetylation across breast cancer tissues, particularly in T47D and MCF-7 cells. Notably, 18 varieties acetyltransferases or deacetylases were identified in T47D cells, among which p300 and Sirtuin3 were validated for their interaction with PGK1. Acetylation at 323 K enhanced PGK1's metabolic role by boosting its activity, glucose uptake, ATP production, and lactate output. This modification also promoted cell proliferation, as evidenced by increased viability, S phase ratio, clonality, and PCNA levels. Furthermore, PGK1-323 K acetylation facilitated metastasis, improving wound healing, cell invasion, and upregulating MMP2, MMP9, N-cadherin, and Vimentin while downregulating E-cadherin.

Conclusion PGK1-323 K acetylation was significantly elevated in T47D and MCF-7 luminal A breast cancer cells and this acetylation could be regulated by p300 and Sirtuin3. PGK1-323 K acetylation promoted cell glycolysis, proliferation, and metastasis, highlighting novel epigenetic targets for breast cancer therapy.

Keywords Breast cancer, PGK1 acetylation, Glycolysis, Cell proliferation and metastasis, Acetyltransferase and deacetylase

*Correspondence:
Yunlong Liu
38396193@qq.com
Liling Yue
yuell1025@126.com
Full list of author information is available at the end of the article

Introduction

Recent global statistics highlight breast cancer as a leading health challenge, with it being the most common cancer in 150 out of 185 countries and holding the highest mortality rate in 110 countries [1]. Particularly concerning is the trend towards younger onset ages, amplifying the urgency for identifying novel targets and developing effective treatments [2]. Breast cancer arises from a complex interplay of factors, with genetic and epigenetic changes playing crucial roles in driving unchecked cell proliferation and survival [3]. While significant strides have been made in understanding genetic contributions to breast cancer, including the identification of pivotal genes like BRCA1, BRCA2, and TP53, many challenges remain. This underscores the importance of exploring epigenetic modifications as potential therapeutic avenues.

Protein post-translational modifications (PTMs) significantly influence protein function by adding chemical groups such as acetyl, phosphoryl, and succinyl groups after translation [4]. Acetylation, initially recognized for modifying histones over sixty years ago, has been extensively studied for its role in regulating gene expression [5]. Beyond histones, acetylation of non-histone proteins is known to impact a wide array of cellular functions, including protein localization, stability, activation, and interaction, thereby influencing key biological processes like cell cycle regulation, DNA damage repair, and metabolism [6–9]. Aberrations in protein acetylation patterns are linked to various diseases, including cancer.

Non-histone proteins offer a greater diversity and abundance compared to histones, opening up wider opportunities for identifying relevant therapeutic targets. Advances in acetylome technology, facilitated by high-resolution mass spectrometry and the use of anti-acetyl-lysine antibodies for protein enrichment, have significantly broadened the scope of acetylated proteins under investigation. This expansion has extended the catalog of acetylated proteins from a limited number of histones to over 2,000 human proteins [10, 11]. Utilizing this technology, studies have explored the acetylation patterns characteristic of various cancers, including pancreatic cancer [12], acute myeloid leukemia [13], cervical cancer [14], and nonfunctional pituitary neuroendocrine tumors [15]. Specifically in breast cancer, comprehensive analysis of tumor xenograft tissue has identified 6,700 acetylation sites across 2,300 proteins, uncovering a wealth of potential targets [16]. However, this wealth of data highlights a gap in comparative studies between cancerous and normal mammary epithelial tissues, as well as a need for further bioinformatic analysis and experimental validation. Therefore, a systematic exploration of proteins acetylated in a breast cancer-specific manner is essential to pinpoint effective targets for therapy.

Our current findings, leveraging proteomic analyses, highlight the metabolic roles of these acetylated proteins, particularly pointing to the glycolytic enzyme phosphoglycerate kinase-1 (PGK1) as a notable target due to its elevated acetylation. We observed an increased expression and specific acetylation of PGK1 at the 323rd lysine residue in breast cancer samples, notably in T47D and MCF-7 cells and also uncovers the regulatory role of p300 and Sirtuin3 in PGK1 acetylation, evidenced by their interaction with PGK1 and altered expression in T47D cells. PGK1-323 K acetylation enhances PGK1's catalytic function, leading to increased glucose metabolism, ATP production and lactate output. Furthermore, PGK1 acetylation was found to bolster cell proliferation and metastasis, as indicated by improved cell viability, cell cycle progression, clonality, wound healing, cell invasion, and upregulating proliferating cell nuclear antigen (PCNA), Matrix Metalloproteinase-2 (MMP2), Matrix Metalloproteinase-2 (MMP9), N-cadherin, and Vimentin while downregulating E-cadherin. These insights contribute to our understanding of protein acetylation's impact on breast cancer, positioning PGK1 acetylation as a promising target for therapeutic intervention and the development of anti-cancer drugs.

Materials and methods

Bioinformatic analysis

Gene Ontology (GO) annotations for acetylated proteins were obtained from the UniProt-GOA database. Initially, identified protein IDs were converted to UniProt IDs and subsequently mapped to GO IDs. For proteins not annotated in the UniProt-GOA database, InterProScan software was employed to assign GO functions based on a protein sequence alignment method. The proteins were then categorized into two GO categories: biological process and molecular function.

Venn analyses to identify overlaps between proteins involved in metabolic processes and those with catalytic functions were conducted using Fun_Rich software (Version 3.1.4). UniProt IDs of the proteins from both groups were uploaded into the software, and Venn analyses were performed to detect proteins present in both groups.

Furthermore, biological process enrichment analysis was carried out for 50 catalytic proteins using the same version of Fun_Rich software. The UniProt IDs of these proteins were uploaded, and enrichment analysis against the background of the UniProt database was performed. Entries yielding a corrected p-value less than 0.05 were deemed to show significant enrichment.

Samples acquisition

Breast cancer specimens and adjacent non-cancerous tissues were obtained from the Second Affiliated Hospital of Qiqihar Medical University. Patient inclusion criteria, along with the procedures for sample collection and preservation, adhered to previously established protocols and complied with the Helsinki Declaration [17]. The Qiqihar Medical Ethics Committee granted approval for all experimental protocols under approval No. [2019]14. Informed consent was obtained from all participants prior to sample collection.

Cell culture and transfection

Cells were maintained as per standard protocols. MCF-10A cells were cultured in MEGM BulletKit (LONZA, CC-3151&CC-4136). Bcap37, ZR-75–1 and MNK45 cells were both cultured in RPMI 1640 medium (HyClone, SH30809.01B) supplemented with 10% fetal bovine serum (FBS) (HyClone, SH30396.03), with ZR-75–1 cells also requiring an addition of 2.5 g/L glucose (Sigma-Aldrich, 158,968) and 0.11 g/L sodium pyruvate (Sigma-Aldrich, I-034). MDA-MB-231 cells were cultured in L15 medium (Biosharp, BL313A) with 10% FBS; A549 cells were cultured in F-12 K medium (Gibco, 21,127,022) with 10% FBS; T47D and Hela cells were maintained in DMEM (HyClone, SH30022.01B) supplemented with 10% FBS. BT-549 and MCF-7 cells followed previously established protocols [17]. All cell lines, except for MDA-MB-231 which does not require CO_2, were incubated in a 5% CO_2 atmosphere at 37℃.

Lentiviral vectors expressing wild type PGK1 (PGK1-WT), a lysine-to-arginine mutant (PGK1-K323R) that cannot be acetylated, a lysine-to-glutamine mutant (PGK1-K323Q) mimicking acetylation, a PGK1 knocking down Sh-RNA sequence (Sh-PGK1), along with corresponding control vectors (NC or Sh-NC), were constructed by GenePharma Co., Ltd (complete sequences were shown in Additional file 1). T47D cells were transfected with these lentiviruses at a multiplicity of infection (MOI) of 50, supplemented with 5ug/mL polybrene. After 72 h, transfected cells were selected using 1ug/mL puromycin to screen successfully transduced cells.

Real-time PCR for PGK1 mRNA expression level

Approximately 1×10^6 MCF-10A and various breast cancer cells were harvested and lysed in 1 mL TRIzol for RNA isolation. Total RNA extracted was reverse transcribed to cDNA using the PrimeScript™ RT Reagent Kit (Takara, RR037A) following the manufacturer's guidelines. The PCR mix was then prepared with TB Green Premix Ex Taq (Takara, RR420A), containing 0.25U DNA polymerase, 150 μg of cDNA, 0.2 mM of each forward and reverse primer, and 1×PCR buffer, topped up with ddH2O to a final volume of 10 μl. The PCR cycling conditions were initiated at 95℃ for 30 s, followed by 40 cycles of 95℃ for 5 s and 60℃ for 30 s, concluding with a final extension that gradually increased from 65℃ to 95℃ at a rate of 0.5℃ per second to generate the melt curve. Details of primers utilized are available in Table 1.

Western blotting

Western blotting process was exerted as before [17]. Related antibodies and dilution ratio were as follows: PGK1 (Santa Cruz, sc-130335, 1:1000), Pan-acetylation (Cell Signaling Technology, 9441, 1:1000), β-actin (Cell Signaling Technology, 4970, 1:1000), FLAG (Sigma, F7425, 1:1000), PCNA(Cell Signaling Technology, 13,110, 1:1000), MMP2 (Cell Signaling Technology, 40,994, 1:1000), MMP9 (Cell Signaling Technology, 13,667, 1:1000), E-cadherin (Proteintech, 20,874–1-AP, 1:2000), N-cadherin (Proteintech, 22,018–1-AP), Vimentin (Proteintech, 10,366–1-AP), HAT1 (PTM Biotechnology, PTM-5195, 1:1000), p300 (Cell Signaling Technology, 70088S, 1:1000), Sirtuin3 (Cell Signaling Technology, 5490S, 1:1000).

Co-immunoprecipitation (Co-IP)

Approximately 5×10^6 cells were lysed in 1 ml of RIPA buffer (Beyotime, P0013B) for protein extraction. To each 500 μg of extracted protein, 5 μg of either capture antibody or species-matched IgG (Beyotime) was added. Samples were incubated overnight at 4℃ with rotation. Subsequently, 20 μl of Protein A/G beads (Santa Cruz, sc-2003) were introduced to each sample and incubated for an additional 90 min. Following incubation, samples were centrifuged at 3000 rpm for 3 min. The resulting pellets were washed six times with cold RIPA buffer and then resuspended in 1×loading buffer. The resuspended samples were boiled for 10 min, after which Western blot analysis was conducted to assess the amounts of specific proteins.

Table 1 Forwards and reverse primer sequences used in RT-PCR experiments

Primer	Sequence (5′—3′)
PGK1-Forward Primer	GTGAAGATTACCTTGCCTGTT
PGK1-Reverse Primer	GCTTCCCATTCAAATACCC
β-actin-Forward Primer	CTGGGCGGGAACTGCCTGACTA
β-actin -Reverse Primer	ACCGCTCGTTGCCGATGGTG

PGK1 activity assay

T47D and MCF-7 cells, transfected with either NC, PGK1-WT, or PGK1-K323R, were harvested for the PGK1 activity assay using the Human PGK1 ELISA Kit (Jianglai Biotechnology, JL14940). Approximately 5×10^5 cells were resuspended in 500 µl of PBS and subjected to protein extraction via repeated freeze–thaw cycles. Post-centrifugation, 50 µl of each cell and standard sample were transferred to plates pre-coated with a PGK1 capture antibody. Subsequently, 100 µl of reaction and detection reagent was added to each well and the plates were incubated for 60 min at 37℃. Following incubation, the supernatant was discarded, and the plates were washed five times. Next, 50 µl of TMB soluble substrate was added to each well and the plates were incubated in the dark for 15 min at 37℃. To conclude the assay, 50 µl of stop buffer was introduced to halt the reaction. The optical density was measured at a wavelength of 450 nm using a microplate reader, and PGK1 activity levels were determined based on the standard curve.

Glucose consumption assay

Glucose consumption was measured using the Glucose Contents Detection Kit (JiNing Industrial Co., Ltd). T47D cells transfected with NC, PGK1-WT, or PGK1-K323R were seeded at a density of 2×10^5 cells/well into a 24-well plate and incubated for 72 h. Subsequently, the supernatant was collected and centrifuged at 5000 rpm for 5 min. A volume of 10 µl from each supernatant, along with 10 µl of ddH2O (for blank) and 10 µl of the standard sample, were allocated to separate wells in a 96-well plate. To each well, 20 µl of Reagent I and 170 µl of Reagent II were added, followed by incubation in the dark at 37℃ for 30 min. The absorbance was measured at 520 nm using multifunctional microplate reader (Tecan Infinite 200 PRO), and glucose consumption was calculated using the formula: 12.49—[(AD—AB)÷(AS—AB)×500÷180.16÷20×100], where 12.49 represents the initial glucose content (in µmol), AD is the absorbance of the sample, AB is the absorbance of the blank, AS is the absorbance of the standard sample, 500 is the total volume of the sample (in µl), 180.16 is the molecular weight of glucose (in ug/umol), and 20 refers to the total number of cells (in 10^4 units).

ATP contents assay

ATP levels were assessed using the Enhanced ATP Assay Kit (Beyotime, S0027), following the manufacturer's guidelines. T47D cells, transfected with NC, PGK1-WT, or PGK1-K323R, numbering 6×10^5, were lysed in 300 µl of extraction buffer and chilled on ice for 5 min. The lysates were centrifuged at 12,000 rpm for 5 min at 4 °C, and the resulting supernatant was used for ATP measurement. A white 96-well plate was prepared, with 100 µl of detection reagent added to each well. The plate was allowed to sit at room temperature for 3–5 min to deplete any background ATP. Subsequently, 20 µl of either the cell lysate or standard samples were dispensed into the wells. The luminescence was quantified using a multifunctional microplate reader (Tecan Infinite 200 PRO), and ATP concentrations were determined based on the standard curve.

Lactic acid assay

Lactic acids were assessed using the Lactic Acid Assay Kit (Solarbio Science & Technology Co., Ltd, BC2235), following the manufacturer's guidelines. T47D cells, transfected with NC, PGK1-WT, or PGK1-K323R, numbering 0.5×10^6, were lysed in 100 µl of extraction buffer I and treated with 300 V ultrasound for 3 min, among which running for 3 s and stopping for 7 s. Centrifuged at 12,000 rpm for 10 min at 4 °C and added 150ul extraction buffer II to 80ul of the supernatant. 30 µl of above supernatant (for experiment group), along with 30 µl of ddH_2O (for blank) and 30 µl of the standard sample were allocated to 1.5 mL centrifugal tube. To each tube, 120ul of reagent I, 30ul of reagent II, and 60ul of reagent IV were added, followed by incubation at 37℃ for 30 min. After that, 18ul reagent V and 180ul reagent III were added and continuously cultured for another 20 min at 37 ℃ in the dark. After the reaction, centrifuged the tubes at 10000 rpm for 10 min and discarded the supernatant. 600ul of absolute ethanol was added to dissolve the precipitates and every 200ul was added to three 96 wells respectively. Finally, detected the absorbance at a wavelength of 570 nm using a multifunctional microplate reader (Tecan Infinite 200 PRO). The lactic acid production was calculated using the formula: $C\div[(N\div V1\times V2)\div(V2+V3)]\times100=575C$ µmol/10^6 cells, where C represent the lactate concentrations of samples (calculated through the absorbance values and the standard curve formulas, in µmol/µl), N is total number of cells (0.5 in 10^6 units), V1 is the volume of extraction buffer I (100 in µl), V2 is the volume of extraction buffer I used for mixing with extraction buffer II (80 in µl), V3 is the volume of extraction buffer II (150 in µl).

CCK8 cell viability assay

Cell viability was assessed using the CCK8 assay. T47D and MCF-7 cells transfected with NC, PGK1-WT, or PGK1-K323R lentiviral vectors, and T47D cells transfected with Sh-PGK1 or Sh-NC lentiviral vectors were plated at a density of 1×10^4 cells/well in a 96-well plate. The cells were incubated for durations of 0, 24, 48, and 72 h, after which 10 µl of CCK8 solution (MCE, HY-K0301) was added to each well, followed by a further

4-h incubation. Absorbance was measured at 450 nm using a multifunctional microplate reader (Tecan Infinite 200 PRO). Cell proliferation rates at each time point, denoted as Xh, were determined by the formula: [(Xh OD value / 0 h OD value)—1] × 100%.

Cell cycle analysis by flow cytometry

Approximately 5×10^5 T47D cells transfected with NC, PGK1-WT, or PGK1-K323R were plated in a 6-well plate and incubated for around 14 h. Subsequently, the supernatant was removed, and the cells were cultured in medium containing 0.1% FBS for 24 h to synchronize them in the G1 phase. The medium was then replaced with one containing 10% FBS, and cells were cultured for an additional 24 h. Cells were harvested and fixed in pre-chilled 70% ethanol. After centrifugation, cells were stained with 200 µl of cell cycle reagent (Muse, MCH100106) for 30 min at room temperature in darkness. Analysis was performed using a Guava Muse Cell Analyzer, and results were processed with FlowJo software (version 10.0).

Colony formation assay

T47D cells transfected with NC, WT-PGK1 or PGK1-K323R, at a density of 500 cells per well, were cultured in a 6-well plate for approximately 15 days. The culture medium was refreshed every three days, and clone formation was monitored using a microscope. Upon observing that most colonies consisted of over 50 cells, the cells were fixed with 4% paraformaldehyde and stained with 0.01% crystal violet. Microscopic images were captured to document clone formation, and the number of clones was counted. This procedure was repeated three times for each group.

Wound healing assay

Approximately 1×10^6 T47D cells, which were transfected with either WT-PGK1, PGK1-K323R or PGK1-K323Q and pre-treated in culture medium without FBS for 24 h, were plated in a 12-well plate and incubated for 24 h. Subsequently, a 10 µl pipette tip was used to create three uniform scratches across the cell monolayer, followed by washing the cells three times with PBS. Each well was then supplemented with 500 µl of culture medium containing 0.1% FBS and incubated for additional periods of 24 and 48 h. Microscopic images were captured at each time point, and the wound healing areas were quantitatively analyzed using Carl Zeiss ZEN software.

Transwell assay

The matrix gel (Beyotime, C0372) was diluted with PBS at a 1:8 ratio and 50 µl of the diluted matrix gel was applied to the upper chamber of a Transwell apparatus. The matrix gel was allowed to solidify for 2 h at 37 °C, followed by the addition of 100 µl of medium containing 0.1% FBS to hydrate the matrix gel for another 30 min at 37 °C. T47D cells, transfected with either WT-PGK1, PGK1-K323R or PGK1-K323Q and pre-treated in culture medium without FBS for 24 h, were then prepared in culture medium with 0.1% FBS at a concentration of 1×10^6 cells/ml. A 100 µl aliquot of such cell suspension was added to the upper chamber, while the lower chamber was filled with culture medium containing 20% FBS. After a 48-h incubation, the cells that had migrated through the matrix were stained with 0.01% crystal violet, and non-migratory cells remaining in the upper chamber were carefully removed. Migrated cells were observed and counted in five randomly selected fields under a microscope.

Proteomic analysis

For proteomic profiling, 1×10^7 MCF-10A and T47D cells were harvested. The processes of protein extraction, digestion, tandem mass tag (TMT) labeling, peptide separation, MS/MS analysis, and database searches were conducted by PTM Biotechnology (Hangzhou, China), following previously established protocols [17]. Data reproducibility analysis was shown in Additional file 2, and the heatmaps for acetyltransferase and deacetylase expression were generated using online tools available on the PTM cloud platform.

Statistical analysis

Enrichment analysis was conducted utilizing Fisher's exact test with adjustments for multiple comparisons through the Benjamini and Hochberg correction (BH method). Comparisons of mean values between two groups were analyzed using the Student's t-test. Statistical significance thresholds were established at * $P < 0.05$ and ** $P < 0.01$, with error bars representing the standard deviation.

Results

Metabolic implications of acetylated proteins in breast *cancer* identified by bioinformatics

Proteomic analyses revealed differential acetylation levels across proteins in breast cancer, with 170 lysine sites on 113 proteins exhibiting elevated acetylation (fold change ≥ 1.5). In contrast, reduced acetylation (fold change ≤ 0.67) was only observed at 33 lysine sites across 13 proteins[17]. These findings underscore the pivotal role of acetylated proteins in breast cancer oncogenesis and progression. Therefore, our initial bioinformatic analysis focused on highly acetylated proteins to identify potential therapeutic targets (Fig. 1A). Among these 113 candidates, 83 proteins were associated with metabolic

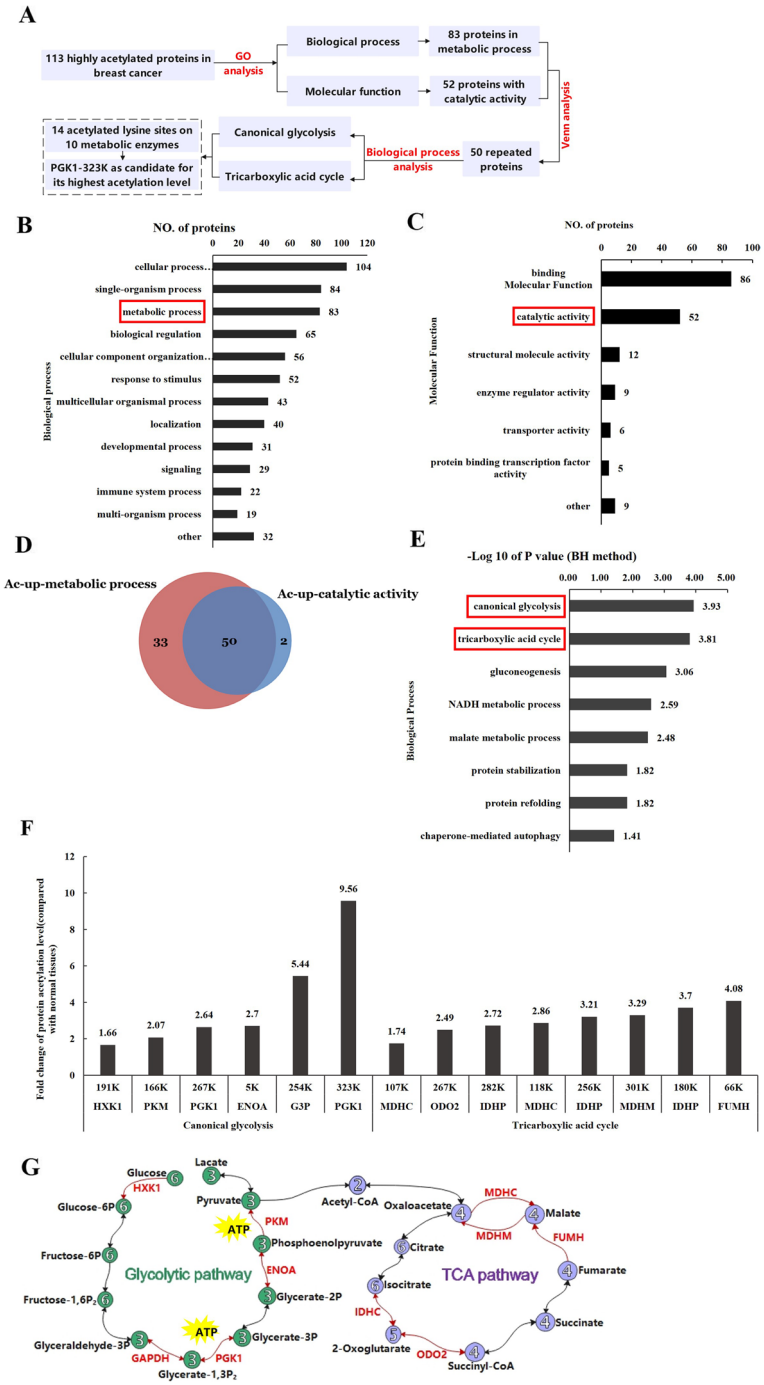

Fig. 1 Bioinformatics Analysis of Acetylated Proteins in Breast Cancer. **A** Flow diagram of the bioinformatic analysis. **B** Distribution of highly acetylated proteins across biological processes. **C** Distribution of highly acetylated proteins by molecular function. **D** Venn diagram illustrating the overlap between proteins involved in metabolic processes (from Fig. 1B) and those with catalytic activities (from Fig. 1C). **E** Enrichment analysis of proteins recurring in Fig. 1D, highlighting their biological processes. **F** Identification of specific proteins and their acetylation sites involved in the glycolysis and tricarboxylic acid (TCA) cycle, as derived from Fig. 1E. **G** Distribution of identified proteins within the glycolysis and TCA cycle pathways. Red fonts represented metabolic enzymes which were highly acetylated

processes, and 52 exhibited catalytic functions (Fig. 1B-C, detailed protein list is available in Additional file 3). Considering that enzymes in metabolic process possess catalytic activity, we hypothesis that the 52 of proteins with catalytic activity could be catalytic enzymes in metabolic process. As predicted, Venn diagrams further confirmed that 50 of these proteins (shown in Additional file 4) are involved in metabolic activities, highlighting their importance as acetylated targets in breast cancer (Fig. 1D). Specifically, biological process analysis of these proteins revealed that they are predominantly involved in glycolysis and the tricarboxylic acid (TCA) cycle (Fig. 1E, specific proteins in each biological process were shown in Additional file 5), with 14 lysine sites on 10 metabolic enzymes undergoing acetylation (Fig. 1F), all the acetylated enzymes (marked in red font) and their locations in corresponding pathways were shown in Fig. 1G. Notably, PGK1 emerged as a critical enzyme with the highest acetylation at lysine 323 (K323), marking a significant fold change of 9.56 (Fig. 1E). Given PGK1's central role in glycolysis and ATP production, and its previously documented involvement in promoting proliferation and tumorigenesis in liver cancer, we selected PGK1-323 K for in-depth investigation in the context of breast cancer, where its role remains to be elucidated.

Elevated expression and acetylation of PGK1 in breast *cancer*

As the substrate of acetylation, the higher expression of protein itself often leads to its higher modification level. Thus, we firstly examined the expression level of PGK1 in different breast cancer tissues and breast cancer cell lines. Western blot analysis revealed that, relative to adjacent non-cancerous tissues, 6 out of 8 breast cancer samples exhibited a higher PGK1 expression level (Fig. 2A), with the quantification of these changes depicted in Fig. 2B. Furthermore, when compared to the normal mammary epithelial cell line MCF-10A, a significant increase in PGK1 mRNA expression was observed in various breast cancer cell lines, including Bcap37, BT-549, ZR-75–1, MCF-7, and T47D (Fig. 2C). This trend of elevated protein expression was consistent across these cancer cell lines, except for MCF-7 and MDA-MB-231 (Fig. 2D), and the detailed fold change quantifications are shown in Fig. 2E. Investigations into the acetylation status of proteins corresponding in molecular weight to PGK1 identified an upregulation in several breast cancer cell lines, particularly in MDA-MB-231, MCF-7, and T47D (Fig. 2D), with T47D cells displaying the highest acetylation levels (Fig. 2E). Recognizing that PGK1 acetylation has been previously identified in other types of cancer, we extended our analysis to include different cancer cell lines—MNK45 (gastric), A549 (lung), and HeLa (cervical)—to assess how their PGK1 acetylation levels compare to those in T47D cells. The findings revealed that T47D cells exhibit significantly higher PGK1 acetylation levels than the other cancer cell lines tested (Fig. 2F-G), indicating that PGK1 acetylation prone to exert its function in breast cancer. These comprehensive analyses indicate a notable upregulation of PGK1 expression and acetylation in breast cancer, pointing towards its potential significance in the disease's molecular dynamics.

Validation of PGK1 lysine 323 acetylation in breast *cancer* cells

Given the observed increase in PGK1 expression and acetylation levels, T47D and MCF-7 cells were selected for detailed validation. Acetylome analysis highlighted significantly enhanced acetylation at the lysine 323 site of PGK1. To investigate this specific site, we generated both the wild type PGK1 (WT-PGK1) and a mutant form (PGK1-K323R), where lysine was replaced by arginine to prevent acetylation. Western blot analysis revealed a marked increase in acetylation levels upon transfection with WT-PGK1, while mutation to arginine led to a notable reduction in acetylation both in T47D (Fig. 3A-B) and MCF-7 cells (Fig. 3C-D). Co-IP further confirmed these findings: mutation of lysine 323 to arginine significantly reduced PGK1 acetylation levels (Fig. 3E-H). These results collectively confirm the specific acetylation of PGK1 at the lysine 323 site.

PGK1 acetylation could be regulated by p300 and Sirtuin3

Protein acetylation is dynamically controlled by acetyltransferases and deacetylases, playing a crucial role in modulating protein function. Our proteomic analysis in T47D and MCF-10A cells identified 18 varieties of these enzymes, indicating a complex regulatory network (Fig. 4A). Notably, histone acetyltransferases (HAT) including HAT7, HAT8, HAT1, and p300 were found to be upregulated in T47D cells (fold change $\geq$ 1.5), hinting at their potential role in enhancing PGK1 acetylation (Fig. 4B). Conversely, while histone deacetylase (HDAC) family members, including HDAC1, HDAC3 and HDAC6, did not show a significant decrease (Fig. 4C). However, Sirtuin family members, particularly Sirtuin7 and Sirtuin3, were expressed at lower levels in T47D cells, suggesting a predominant role of Sirtuins in PGK1 deacetylation (Fig. 4C). The use of Nicotinamide (NAM), a Sirtuin inhibitor, led to a marked increase in PGK1 acetylation in cells overexpressing WT-PGK1, further implicating Sirtuins in the regulation of PGK1 acetylation (Fig. 4D, E). Validation efforts focused on the most significantly altered regulators through Western blot analysis revealed that HAT1, p300, and Sirtuin3 showed corresponding differential expression between MCF-10A

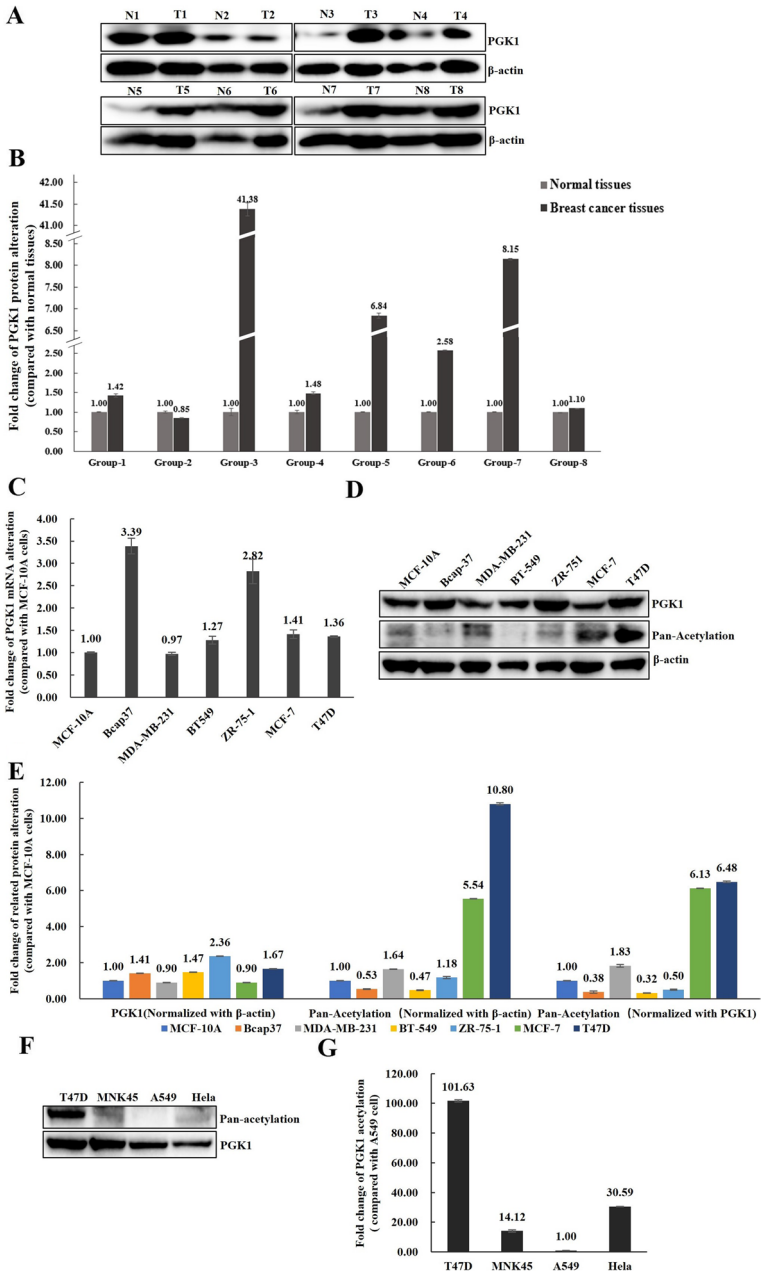

Fig. 2 Evaluation of PGK1 Expression and Acetylation in Breast Cancer. **A** Western blot analysis showing PGK1 expression in breast cancer and adjacent non-cancerous tissues, with β-actin serving as the loading control. **B** Quantitative analysis of the data presented in Fig. 2A. **C** Real-time PCR assessment of PGK1 mRNA levels in various breast cancer cell lines compared to MCF-10A (the results showed the relative fold changes), using β-actin as the normalization reference. **D** Western blot examination of PGK1 protein levels and acetylation status in breast cancer cell lines versus MCF-10A, with β-actin as the normalization reference. **E** Quantitative analysis of the data shown in Fig. 2D. **F** Western blot analysis comparing PGK1 protein levels and acetylation across different cancer cell types, utilizing PGK1 itself for normalization. **G** Quantitative analysis of Fig. 2F, displaying fold changes in PGK1 acetylation relative to A549 cells, identified as having the lowest level of acetylation

and T47D cells, aligning with their proposed regulatory roles (Fig. 4F). Co-IP experiments further supported this, demonstrating the interactions between PGK1 and both p300 and Sirtuin3 but not with HAT1 (Fig. 4G). These findings collectively suggest that PGK1 acetylation is modulated by specific acetyltransferases and deacetylases, with p300 and Sirtuin3 playing pivotal roles in this regulatory mechanism.

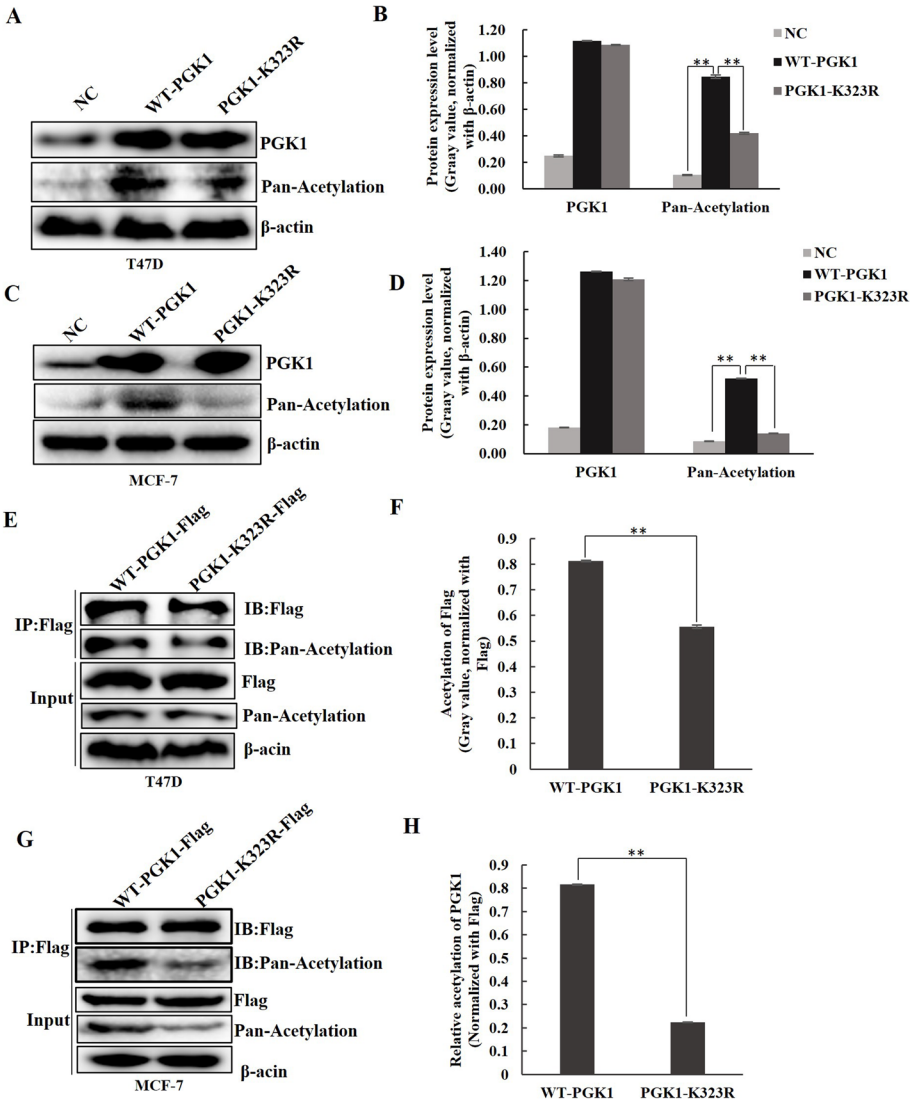

Fig. 3 Confirmation of Acetylation at PGK1 Lysine 323 in T47D and MCF-7 Cells. **A**, **C** Western blot analysis showing PGK1 protein levels and acetylation in T47D (**A**) and MCF-7 (**C**) cells transfected with wild type PGK1 (WT-PGK1), a non-acetylatable mutant (PGK1-K323R, with lysine mutated to arginine), and the control vector (NC), with β-actin as the loading control. **B**, **D** Quantitative analysis of PGK1 expression and acetylation levels from Fig. 3A and C. **E**, **G** Co-IP assay detecting PGK1 acetylation in T47D (**E**) and MCF-7 (**G**) cells transfected with either WT-PGK1 or PGK1-K323R mutant, using FLAG as the Co-IP loading control and β-actin for the input control. **F**, **H** Quantitative analysis of Co-IP results from Fig. 3E and G

(See figure on next page.)

Fig. 4 Identifying and Validating Regulators of PGK1 Acetylation. **A** Overview of acetyltransferases and deacetylases identified in MCF-10A and T47D cells via proteomic analysis. **B** Comparison of acetyltransferase expression levels in T47D cells relative to MCF-10A cells, with MCF-10A expression levels set as the baseline (1.0). **C** Comparison of deacetylase expression levels in T47D cells relative to MCF-10A cells, with MCF-10A expression levels standardized to 1.0. **D** Western blot analysis illustrating the impact of Nicotinamide (NAM) at concentrations of 25 mM and 50 mM on PGK1 acetylation in T47D cells expressing WT-PGK1. **E** Quantitative analysis of PGK1 acetylation changes depicted in Fig. 4D. **F** Western blot showing expression levels of HAT1, p300, and Sirtuin3 in MCF-10A versus T47D cells, with β-actin serving as the loading control. **G** Co-immunoprecipitation (Co-IP) assays examining interactions between PGK1 and the enzymes p300, Sirtuin3, and HAT1, highlighting the specific regulatory connections

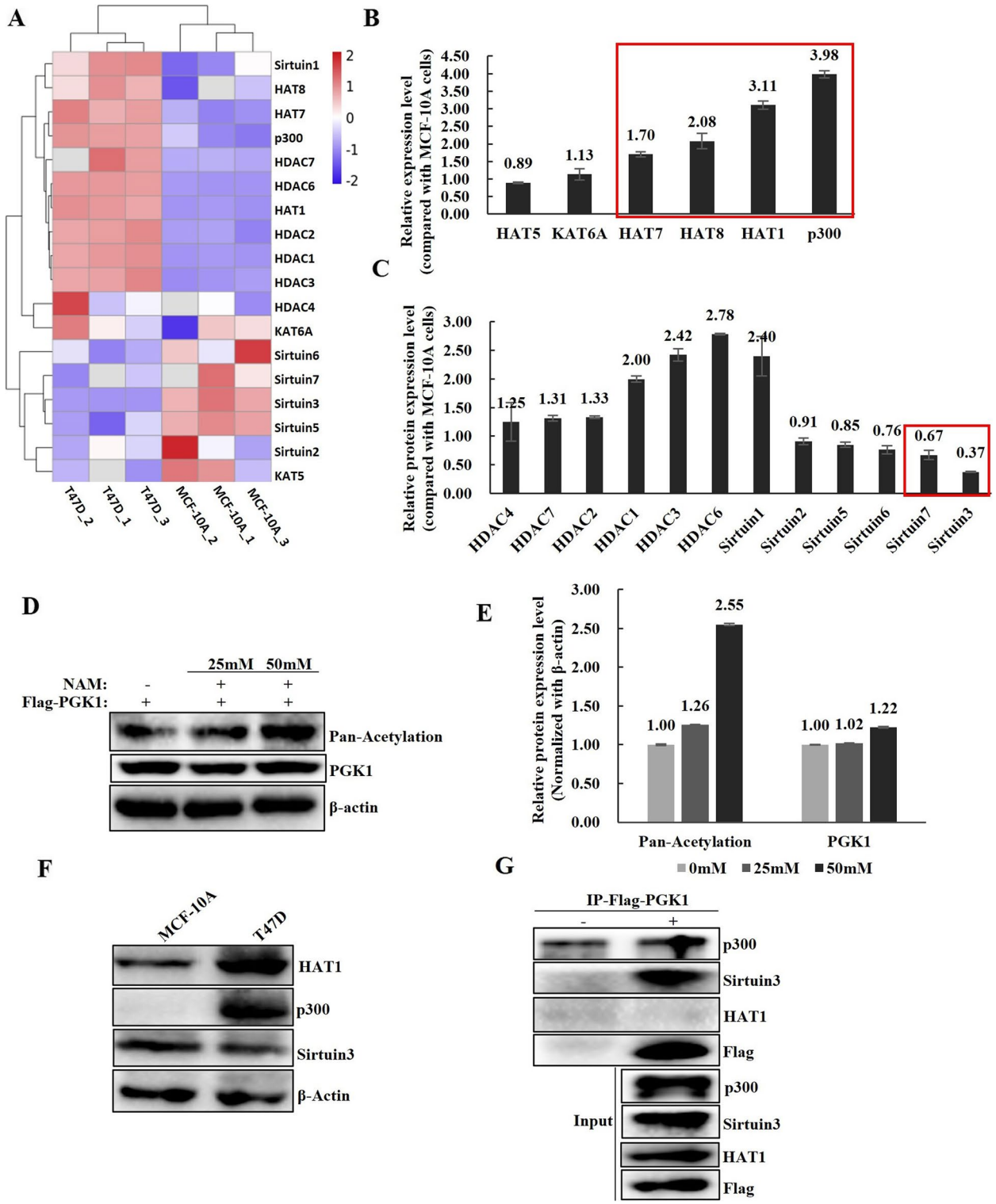

Fig. 4 (See legend on previous page.)

PGK1 lysine 323 acetylation enhances glycolysis in breast *cancer* cells

Acetylome analyses have identified PGK1 as a protein undergoing extensive acetylation at multiple lysine residues [15, 18–22] (Fig. 5A). Despite this knowledge, systematic studies on PGK1 acetylation are limited, with

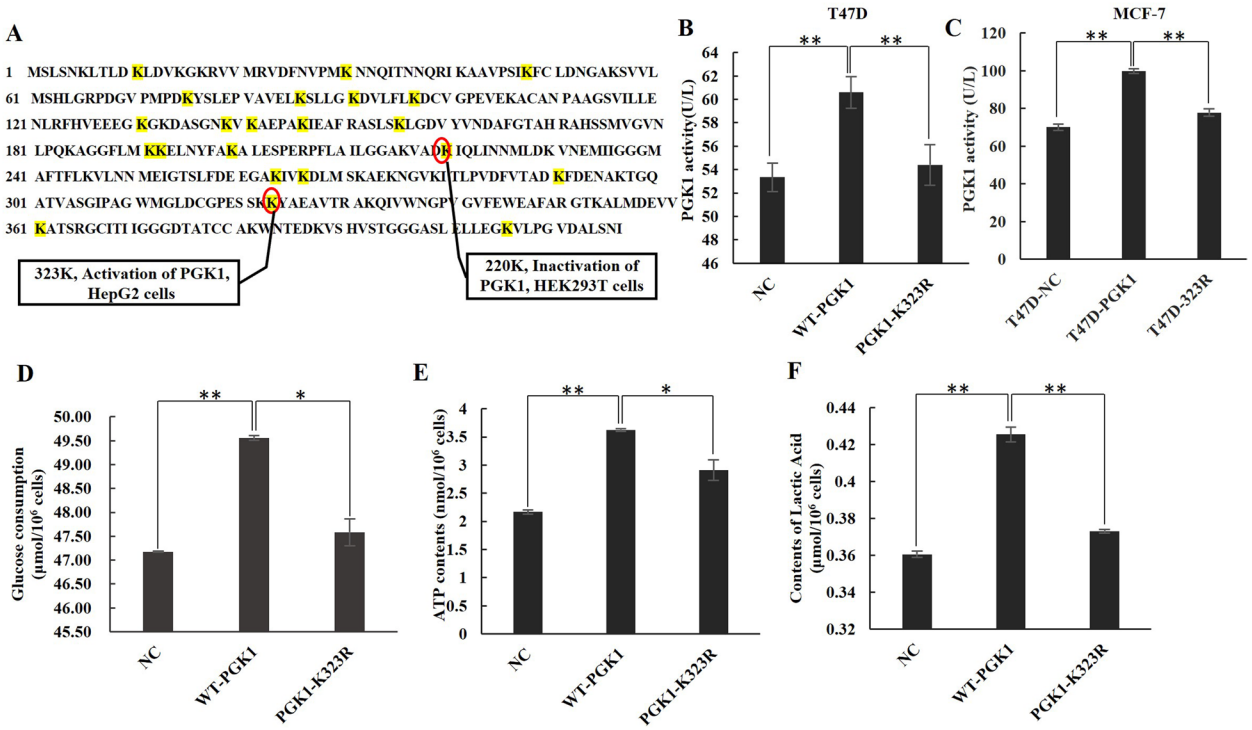

Fig. 5 Effects of PGK1 lysine 323 acetylation on glycolysis pathway. **A** Identified functional implications of acetylated lysine residues on PGK1. **B**, **C** Assessment of PGK1 enzymatic activity in T47D (**B**) and MCF-7 (**C**) cells transfected with wild type PGK1 (WT-PGK1), the non-acetylatable mutant (PGK1-K323R, with lysine mutated to arginine preventing acetylation), or the control vector (NC). **D** Evaluation of glucose consumption in T47D cells expressing wild type PGK1 (WT-PGK1), the non-acetylatable mutant (PGK1-K323R), or the control vector (NC). **E** Measurement of ATP production in T47D cells transfected wild type PGK1 (WT-PGK1), the non-acetylatable mutant (PGK1-K323R), or the control vector (NC). **F** Examination of lactic acid production in T47D cells transfected wild type PGK1 (WT-PGK1), the non-acetylatable mutant (PGK1-K323R), or the control vector (NC)

only two out of four reporting its direct impact on enzymatic activity [18, 19] (Fig. 5A). To elucidate the role of PGK1 acetylation in breast cancer, we first assessed its influence on the enzyme's catalytic function. Transfection with WT-PGK1 led to an increase in PGK1 catalytic activity in T47D and MCF-7 cells, an effect not observed with the acetylation-deficient mutant PGK1-K323R (Fig. 5B, C). As is known to us, PGK1 is an important rate-limiting enzyme in glycolysis pathway which can catalyze ATP production directly. The reason why cancer cells can proliferate rapidly is that they can consume a lot of glucose at a faster rate, and then produce ATP more quickly, which is achieved through the higher enzyme activity in glycolysis pathway. Thus, after the PGK1 activity, we detected the glucose consumption and ATP contents. The results showed that WT-PGK1 increased both glucose consumption and ATP production in T47D cells, whereas these effects were not significant in cells expressing the PGK1-K323R mutant (Fig. 5D, E). Additionally, the PGK1-K323R mutant was found to inhibit lactic acid production (Fig. 5F). These findings collectively demonstrate that PGK1 acetylation facilitates glycolysis, potentially explaining the enhanced glycolytic efficiency observed in tumor cells. This mechanism underscores the importance of PGK1 acetylation in promoting the metabolic adaptations observed in breast cancer cells.

PGK1 lysine 323 acetylation enhances cell proliferation in breast *cancer* cells

The Warburg effect underscores aerobic glycolysis's crucial function in cancer progression, illustrating why cancer cells favor glycolysis for energy production, facilitating proliferation, invasion, and metastasis under aerobic conditions [23, 24]. This preference suggests that PGK1 acetylation might influence these cellular processes in breast cancer. Our findings from the CCK8 assay indicate a significant increase in cell viability (Fig. 6A, C) and proliferation (Fig. 6B, D) in T47D and MCF-7 cells expressing WT-PGK1 at 48- and 72-h post-transfection. In contrast, cells expressing the PGK1-K323R mutant, which lacks acetylation at lysine 323, showed viability and proliferation rates similar to the control group (Fig. 6A-D). Additionally, silencing PGK1 expression markedly reduced cell viability (Fig. 6E) and cell proliferation ratio (Fig. 6F), highlighting its role in cell growth. Further analysis revealed that WT-PGK1

transfection raised the proportion of cells in the S phase from 28.7% to 35.9% and reduced those in the G1 phase from 44.4% to 36.5% (Fig. 6G), indicating an increased number of cells entering the cell cycle. This effect was not observed with the PGK1-K323R mutant (Fig. 6G), suggesting a loss of function due to the absence of acetylation at lysine 323. Moreover, clone formation assays demonstrated that WT-PGK1-transfected cells formed more colonies than those transfected with the control or PGK1-K323R mutant (Fig. 6H, I). Further, the expression level of the proliferation marker PCNA was higher in cells expressing WT-PGK1 compared to those expressing

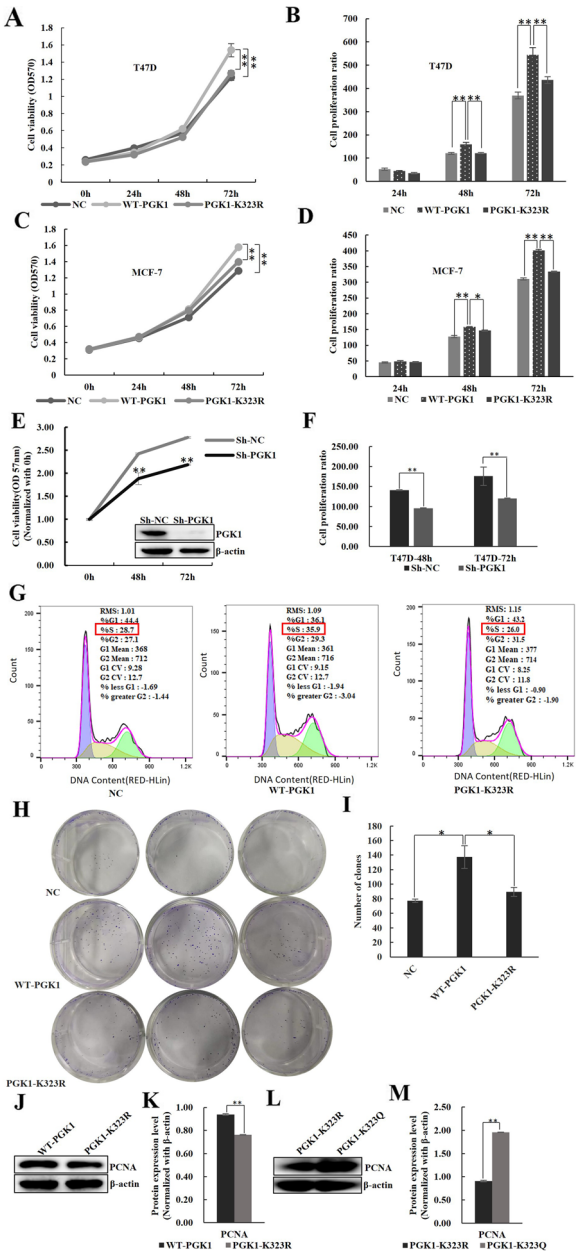

Fig. 6 Effects of PGK1-323 K acetylation on cell proliferation in T47D and MCF-7 cells. **A**, **C** Cell viability assessed by CCK8 assay in T47D (**A**) and MCF-7 (**C**) cells transfected WT-PGK1, PGK1-K323R, or the control vector (NC) over time intervals of 0, 24, 48, and 72 h. **B**, **D** Analysis of T47D (**B**) and MCF-7 (**D**) cell proliferation ratios at 24, 48, and 72 h, normalized to the 0-h measurement. **E** Cell viability assessed by CCK8 assay in T47D cells transfected with the expression vector that can knockdown endogenous PGK1 (Sh-PGK1) or control vector (Sh-Control) over 48 and 72 h. **F** Analysis of cell proliferation ratios at 48 and 72 h, normalized to the 0-h measurement. **G** Evaluation of cell cycle phases in T47D cells expressing WT-PGK1, PGK1-K323R, or NC. **H** Clonogenic assay results in T47D cells transfected with WT-PGK1, PGK1-K323R, or NC to assess the ability to form colonies. **I** Quantitative analysis of clone formation depicted in Fig. 5H. **J** Western blot analysis measuring PCNA levels in T47D cells transfected with WT-PGK1 or PGK1-K323R, with β-actin as the loading control. **K** Quantification of PCNA expression from Fig. 5J. **L** Western blot showing PCNA expression in T47D cells transfected with PGK1-K323R or the acetylation-mimicking mutant PGK1-K323Q, with β-actin serving as the loading control. **M** Quantitative analysis of PCNA levels from Fig. 5L. Notations: WT-PGK1 denotes the wild type form of PGK1; PGK1-K323R refers to a mutant variant where lysine is replaced with arginine, inhibiting acetylation; PGK1-K323Q represents a mutant designed to mimic the acetylated state of lysine 323

the PGK1-K323R mutant (Fig. 6J, K). The PGK1-K323Q mutant, which mimics acetylation at lysine 323, also showed increased PCNA expression compared to the PGK1-K323R mutant (Fig. 6L, M). These comprehensive results establish that acetylation at lysine 323 of PGK1 promotes cell proliferation and may contribute to the metastatic potential of breast cancer cells.

PGK1 lysine 323 acetylation facilitates metastasis in T47D cells

Besides findings related to cell proliferation, we also explored the influence of PGK1 lysine 323 acetylation on metastatic capabilities. Wound-healing assays and Transwell experiments revealed that when compared with wild type PGK1, the non-acetylated PGK1-K323R mutant significantly decreased the wound healing rate and the number of invasive cells (Fig. 7A-D). Similarity results were also observed when compared with the acetylation mimic PGK1-323Q (Fig. 7E-H). These observations indicate that acetylation at PGK1 lysine 323 promotes cellular migration and invasion. Furthermore, Western-blot analysis showed that the PGK1-K323R mutant, in contrast to WT-PGK1 and PGK1-323Q, led to reduced levels of the metastasis-associated markers MMP2 and MMP9, and decreased expression of the mesenchymal markers N-cadherin and Vimentin. Conversely, it increased the expression of the epithelial marker E-cadherin (Fig. 7I-L). Collectively, these findings substantiate the role of PGK1

lysine 323 acetylation in facilitating the metastatic potential of breast cancer cells.

Discussion

This study conducted a comprehensive analysis of acetylated proteins in breast cancer, pinpointing PGK1 lysine 323 acetylation as a significant target. This highlights that even if breast tissue's metabolic activity is not as pronounced as in organs like the liver or heart, aberrant acetylation of metabolic enzymes remains a critical research avenue in breast cancer. Interestingly, PGK1 acetylation levels seems higher in luminal A breast cancer cells (T47D and MCF-7) compared to those in luminal B and basal B types (MDA-MB-231, BT-549, ZR-75–1), suggesting subtype-specific roles. However, specific acetylation situation of PGK1 in different types of breast cancer still needs to be further verified.

In this study, we found that a significant portion (73%, 83 of 113) of acetylated proteins are involved in metabolic processes, with a substantial 60% of these proteins functioning as catalytic enzymes. This observation aligns with the understanding that non-histone acetylation can modulate enzyme activities [25, 26], suggesting its potential role in altering breast cancer metabolism. Although metabolic enzymes represent a significant fraction of acetylated proteins, it's noteworthy that only those with a substantial control over metabolic flux can impact cancer progression when their activities are modified. In contrast, enzymes without control roles appear to have negligible effects [21, 27, 28]. We found that PGK1, which converts 1,3-diphosphoglycerate to 3-phosphoglycerate and directly produces ATP in glycolysis [29], was outstanding by its 9.56-fold increase of acetylation level on 323rd lysine (Fig. 1F). It has been reported that though glycolysis produce much less ATP compared with mitochondrial oxidative phosphorylation, tumor cells develop the methods to enhance the efficiency of glycolysis [30]. Our results may help to explain the mechanism by which tumor cells enhance their glycolytic efficiency.

Beyond PGK1, our investigation uncovered the acetylation of PKM (M type pyruvate kinase), a crucial enzyme in glycolysis facilitating the transfer of a phosphoryl group from phosphoenolpyruvate (PEP) to ADP, thus generating ATP (Fig. 1F/G). Notably, acetylation of PKM2 has been linked to the enhancement of the Warburg effect and nuclear protein kinase activity in hepatocellular carcinoma and glioma, respectively [31, 32]. Moreover, acetylation at PKM2 lysine 305, mediated by SIRT2, was found to inhibit glycolysis and reduce tumor growth in breast cancer [33], suggesting PKM2 acetylation as a potential glycolytic target in breast cancer treatment. Our study also highlights acetylation alterations in various enzymes within the tricarboxylic acid (TCA) cycle (Fig. 1F/G). These modifications have been documented in conditions such as cervical cancer [34], cardiac failure [35], pancreatic cancer [36] and intracerebral hemorrhage [37], but not previously in breast cancer. This gap underscores our findings as a novel contribution, suggesting these acetylated enzymes as potential investigatory targets for breast cancer from a TCA cycle perspective.

In our work, we have established the stimulatory role of the 323rd lysine acetylation on PGK1's functionality, influencing cell growth and metastasis in breast cancer (refer to Figs. 6 and 7). Interestingly, the impact of acetylation on PGK1 varies significantly: while acetylation at the 323rd lysine enhances PGK1's role in liver cancer proliferation, aligning with our findings [18], acetylation at the 220th lysine inhibits its activity by 37%, attributed to its interference with ADP binding [19]. Unlike histone acetylation's generally positive modulation of gene transcription, non-histone protein acetylation effects on enzyme activities exhibit considerable variability across different enzymes, isoforms, and acetylation sites [21]. Predominantly, acetylation tends to inhibit enzyme activities.

The influence of acetylation on proteins can lead to varied outcomes, hinging on several factors: (1) Protein

(See figure on next page.)

Fig. 7 Effects of PGK1-323 K acetylation on metastasis in T47D cells. **A** Wound healing assay in T47D cells transfected with WT-PGK1 and non-acetylatable PGK1-K323R mutant, monitored at 0-, 24-, and 48-h post-scratch. **B** Quantitative analysis of wound closure from Fig. 7A. **C** Transwell invasion assay for T47D cells expressing either WT-PGK1 or PGK1-K323R, evaluated after 48 h of culture. **D** Quantitative results of the invasion assay from Fig. 7C. **E** Wound healing assay in T47D cells transfected with the non-acetylatable PGK1-K323R mutant or the acetylation-mimicking PGK1-323Q mutant, monitored at 0-, 24-, and 48-h post-scratch. **F** Quantitative analysis of wound closure from Fig. 7E. **G** Transwell invasion assay for T47D cells expressing either PGK1-K323R or PGK1-323Q, evaluated after 48 h of culture. **H** Quantitative results of the invasion assay from Fig. 7G. **I** Western blot analysis assessing the levels of metastasis-related markers (MMP9, MMP2) and epithelial-to-mesenchymal transition (EMT) markers (E-cadherin, N-cadherin, Vimentin) in T47D cells expressing WT-PGK1 or PGK1-K323R, with β-actin as the loading control. **J** Quantitative evaluation of protein expression levels from Fig. 7I. **K** Western blot analysis comparing the expression of metastasis and EMT markers in T47D cells transfected with PGK1-K323R or PGK1-K323Q, using β-actin for loading control. **L** Quantification of protein expression from Fig. 7K. WT-PGK1 refers to the wild-type PGK1; PGK1-K323R denotes a mutant variant where lysine is substituted with arginine, inhibiting acetylation; PGK1-K323Q represents a mutant designed to simulate acetylation at lysine 323

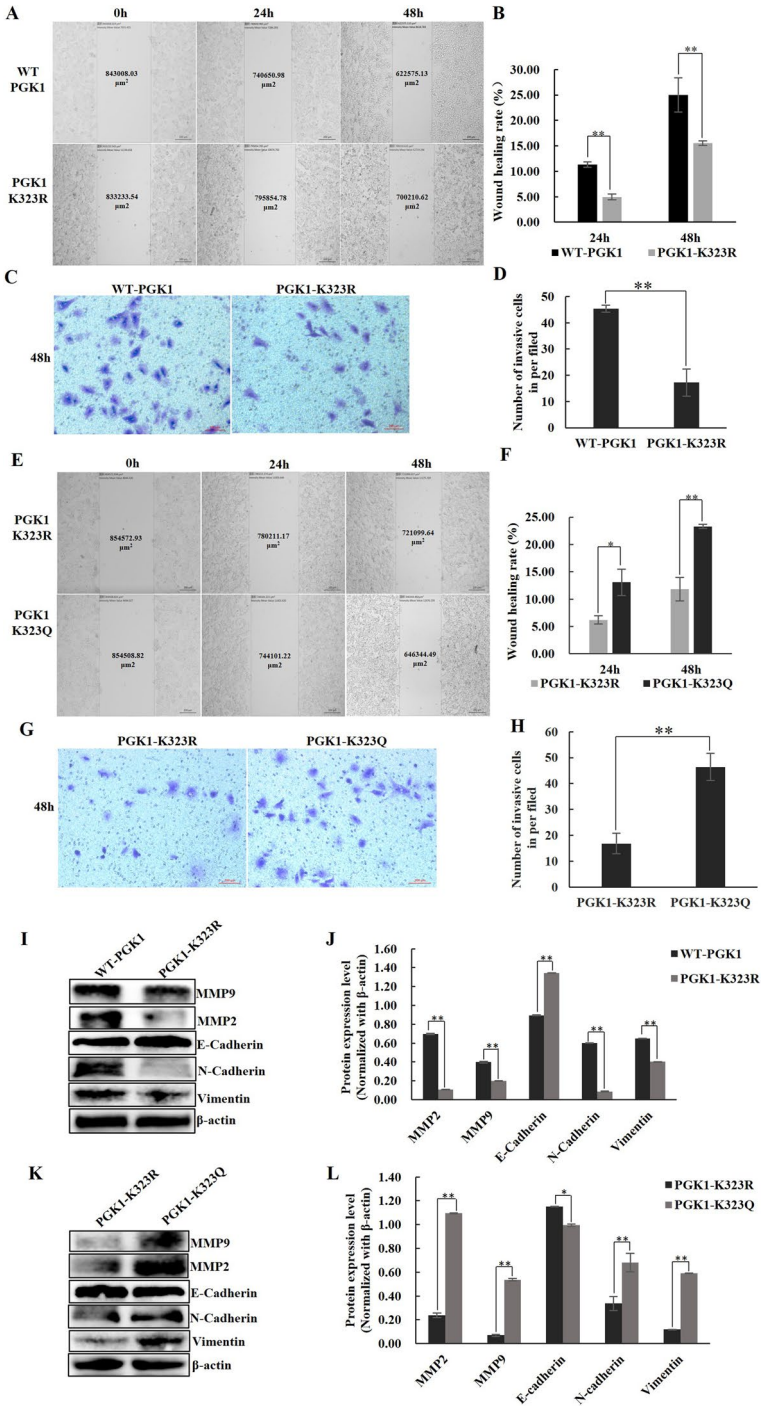

Fig. 7 (See legend on previous page.)

Localization: acetylation can direct proteins between the nucleus and cytoplasm, with cytoplasmic presence typically enhancing metabolic enzyme function. This is due to metabolic activities predominantly occurring in the cytoplasm. For instance, acetylation at lysine 472 on fructose-2,6-bisphosphatase 3 (PFKFB3) hinders its nuclear translocation, fostering its accumulation and activation in the cytoplasm, thereby stimulating glycolysis [38, 39]. Conversely, acetylation at lysine 433 on PKM2 favors its nuclear localization and reduces its enzymatic activity, thus shifting glycolysis towards biomass production and cancer progression [31, 40, 41]. (2) Protein Interactions:

acetylation can also modulate the interactions between proteins, influencing their activities. Acetylation at lysine 220 on PGK1, located at its ADP binding site, impedes its interaction with ADP, reducing PGK1 activity. On the flip side, acetylation enhances the interaction between glutamate oxaloacetate transaminases (GOT) and malate dehydrogenases (MDH), facilitating efficient substrate channeling for the malate–aspartate shuttle and boosting glycolysis [36]. (3) Protein Stability: acetylation can trigger protein degradation, diminishing enzyme activity. This mechanism is exemplified by phosphoenolpyruvate carboxykinase1 (PEPCK1), a crucial enzyme in gluconeogenesis, whose acetylation leads to its degradation, thus potentially regulating gluconeogenesis [42]. These examples underscore the complex regulatory landscape of protein acetylation, with implications for both enzymatic function and broader metabolic pathways.

Therefore, it's crucial to evaluate the impact of non-histone acetylation within its specific context. Beyond acetylation, protein succinylation similarly influences enzyme activities, highlighting the intricate network of post-translational modifications [43–45]. Both acetylation and succinylation processes are modulated by enzymes like HAT2A [46], Sirtuin5 [47–49], and Sirtuin7 [50, 51]. Notably, our findings point to an unusual expression of p300 and Sirtuin3 in T47D cells (refer to Fig. 4), along with their interaction with PGK1, hinting at potential regulators of PGK1 acetylation and deacetylation. This observation merits further exploration to elucidate the underlying mechanisms.

Abbreviations

iTRAQ	Isobaric Tags for Relative and Absolute Quantitation
PTMs	Protein post-translational modifications
TCA	Tricarboxylic Acid
PGK1	Phosphoglycerate Kinase-1
PCNA	Proliferating Cell Nuclear Antigen
MMP2	Matrix Metalloproteinase-2
MMP9	Matrix Metalloproteinase-9
GO	Gene Ontology
MOI	Multiplicity Of Infection
TMT	Tandem Mass Tag
Co-IP	Co-immunoprecipitation
EMT	Epithelial-to-mesenchymal Transition
NAM	Nicotinamide
HAT	Histone Acetyltransferases
HDAC	Histone Deacetylase
PKM	M Type Pyruvate Kinase
PEP	Phosphoryl Group from Phosphoenolpyruvate
PFKFB3	Fructose-2,6-Bisphosphatase 3
GOT	Oxaloacetate Transaminases
MDH	Malate Dehydrogenases
PEPCK1	Phosphoenolpyruvate Carboxykinase1

Supplementary Information

The online version contains supplementary material available at https://doi.org/10.1186/s12885-024-12792-8.

Supplementary Material 1

Supplementary Material 2

Supplementary Material 3

Supplementary Material 4

Supplementary Material 5

Acknowledgements
Not applicable.

Authors' contributions
Xiuli Gao Yunlong Liu and Liling Yue contributed to the conception and design; Ting Pan contributed to the experiments sumpletment after major revision; Yu Gao, Wenbin Zhu and Likun Liu were response for experiment execution; Wenbo Duan and Qiuhang Song contributed to bioinformatic analysis; Cuicui Han and Yunlong Liu contributed to collection of tissue samples; Bo Feng and Wenjing Yan contributed to preparation of materials. The first draft of the manuscript was written by Xiuli Gao and was revised by Liling Yue. All authors read and approved the final manuscript.

Funding
National Natural Science Foundation of China [81972491]; Natural Science Foundation of Heilongjiang Province [YQ2021H028]; Post-doctoral Foundation of Heilongjiang Province [LBH-Z22295]; Education Department of Heilongjiang Province [2021-KYYWF-0337, 2022-KYYWF-0831]; Clinical Research Foundation of Qiqihar Medical University [QMSI2021L-14]; Projects of Hebei Provincial Administration of Traditional Chinese Medicine [2022087].

Availability of data and materials
The datasets generated during the current study are available from the corresponding author upon reasonable request.

Declarations

Ethics approval and consent to participate
This study was performed in line with the principles of the Declaration of Helsinki. Approval was granted by the Ethics Committee of Qiqihar Medical University (NO. [2019]14). Informed consent was obtained from all individual participants included in the study.

Consent for publication
Not applicable.

Competing interests
The authors declare no competing interests.

Author details
[1]Research Institute of Medicine and Pharmacy, Qiqihar Medical University, Qiqihar, Heilongjiang, China. [2]Department of Medical Technology, Qiqihar Medical University, Qiqihar, Heilongjiang, China. [3]The Third Affiliated Hospital of Qiqihar Medical University, Qiqihar, Heilongjiang, China. [4]College of Pharmacy, Qiqihar Medical University, Qiqihar, Heilongjiang, China. [5]Dean's Office, Qiqihar Medical University, Qiqihar, Heilongjiang, China. [6]College of Basic Medicine, Hebei University of Chinese Medicine, Shijiazhuang, China. [7]The Second Affiliated Hospital of Qiqihar Medical University, Qiqihar, Heilongjiang, China.

Received: 2 March 2023 Accepted: 9 August 2024
Published online: 27 August 2024

References

1. Sung H, Ferlay J, Siegel RL, Laversanne M, Soerjomataram I, Jemal A, Bray F. Global Cancer Statistics 2020: GLOBOCAN estimates of incidence and mortality worldwide for 36 cancers in 185 countries. CA Cancer J Clin. 2021;71(3):209–49.
2. Rossi L, Mazzara C, Pagani O. Diagnosis and treatment of breast cancer in young women. Curr Treat Options Oncol. 2019;20(12):86.

3. Feng Y, Spezia M, Huang S, Yuan C, Zeng Z, Zhang L, Ji X, Liu W, Huang B, Luo W, et al. Breast cancer development and progression: risk factors, cancer stem cells, signaling pathways, genomics, and molecular pathogenesis. Genes Dis. 2018;5(2):77–106.
4. Li S, Iakoucheva LM, Mooney SD, Radivojac P. Loss of post-translational modification sites in disease. Pac Symp Biocomput 2010:337–47.
5. Narita T, Weinert BT, Choudhary C. Functions and mechanisms of non-histone protein acetylation. Nat Rev Mol Cell Biol. 2019;20(3):156–74.
6. Schultz-Rogers LE, Thayer ML, Kambakam S, Wierson WA, Helmer JA, Wishman MD, Wall KA, Greig JL, Forsman JL, Puchhalapalli K, et al. Rbbp4 loss disrupts neural progenitor cell cycle regulation independent of Rb and leads to Tp53 acetylation and apoptosis. Dev Dyn. 2022;251(8):1267–90.
7. Zhang T, Wang Z, Liu M, Liu L, Yang X, Zhang Y, Bie J, Li Y, Ren M, Song C, et al. Acetylation dependent translocation of EWSR1 regulates CHK2 alternative splicing in response to DNA damage. Oncogene. 2022;41(29):3694–704.
8. Cheng YW, Zeng FM, Li DJ, Wang SH, He JZ, Guo ZC, Nie PJ, Wu ZY, Shi WQ, Wen B, et al. P300/CBP-associated factor (PCAF)-mediated acetylation of Fascin at lysine 471 inhibits its actin-bundling activity and tumor metastasis in esophageal cancer. Cancer Commun (Lond). 2021;41(12):1398–416.
9. Bazylianska V, Kalpage HA, Wan J, Vaishnav A, Mahapatra G, Turner AA, Chowdhury DD, Kim K, Morse PT, Lee I, et al. Lysine 53 acetylation of cytochrome c in prostate cancer: Warburg metabolism and evasion of apoptosis. Cells. 2021;10(4):802.
10. Gil J, Ramirez-Torres A, Encarnacion-Guevara S. Lysine acetylation and cancer: a proteomics perspective. J Proteomics. 2017;150:297–309.
11. Zrimsek M, Kucharikova H, Draganic K, Dobrovolna P, Heiss Spornberger V, Winkelmayer L, Hassler MR, Lochmanova G, Zdrahal Z, Egger G. Quantitative acetylomics uncover acetylation-mediated pathway changes following histone deacetylase inhibition in anaplastic large cell lymphoma. Cells. 2022;11(15):2380.
12. Yang L, Fu Q, Miao L, Ding Q, Li X, Wang J, Jiang G, Wang Y. Quantitative acetylome and phosphorylome analysis reveals Girdin affects pancreatic cancer progression through regulating Cortactin. Aging (Albany NY). 2020;12(9):7679–93.
13. Zhu X, Liu X, Cheng Z, Zhu J, Xu L, Wang F, Qi W, Yan J, Liu N, Sun Z, et al. Quantitative analysis of global proteome and lysine acetylome reveal the differential impacts of VPA and SAHA on HL60 Cells. Sci Rep. 2016;6:19926.
14. Zhang L, Wang W, Zhang S, Wang Y, Guo W, Liu Y, Wang Y, Zhang Y. Identification of lysine acetylome in cervical cancer by label-free quantitative proteomics. Cancer Cell Int. 2020;20:182.
15. Wen S, Li J, Yang J, Li B, Li N, Zhan X. Quantitative acetylomics revealed acetylation-mediated molecular pathway network changes in human nonfunctional pituitary neuroendocrine tumors. Front Endocrinol (Lausanne). 2021;12;753606.
16. Svinkina T, Gu H, Silva JC, Mertins P, Qiao J, Fereshetian S, Jaffe JD, Kuhn E, Udeshi ND, Carr SA. Deep, quantitative coverage of the lysine acetylome using novel anti-acetyl-lysine antibodies and an optimized proteomic workflow. Mol Cell Proteomics : MCP. 2015;14(9):2429–40.
17. Gao X, Bao H, Liu L, Zhu W, Zhang L, Yue L. Systematic analysis of lysine acetylome and succinylome reveals the correlation between modification of H2A.X complexes and DNA damage response in breast cancer. Oncol Rep. 2020;43(6):1819–30.
18. Hu H, Zhu W, Qin J, Chen M, Gong L, Li L, Liu X, Tao Y, Yin H, Zhou H, et al. Acetylation of PGK1 promotes liver cancer cell proliferation and tumorigenesis. Hepatology. 2017;65(2):515–28.
19. Wang S, Jiang B, Zhang T, Liu L, Wang Y, Wang Y, Chen X, Lin H, Zhou L, Xia Y, et al. Insulin and mTOR pathway regulate HDAC3-mediated deacetylation and activation of PGK1. PLoS Biol. 2015;13(9):e1002243.
20. Huang H, Tang S, Ji M, Tang Z, Shimada M, Liu X, Qi S, Locasale JW, Roeder RG, Zhao Y, et al. p300-Mediated lysine 2-Hydroxyisobutyrylation regulates glycolysis. Mol Cell. 2018;70(5):984.
21. Marin-Hernandez A, Rodriguez-Zavala JS, Jasso-Chavez R, Saavedra E, Moreno-Sanchez R. Protein acetylation effects on enzyme activity and metabolic pathway fluxes. J Cell Biochem. 2022;123(4):701–18.
22. Min Z, Long X, Zhao H, Zhen X, Li R, Li M, Fan Y, Yu Y, Zhao Y, Qiao J. Protein lysine acetylation in ovarian granulosa cells affects metabolic homeostasis and clinical presentations of women with polycystic ovary syndrome. Front Cell Dev Biol. 2020;8:567028.
23. Vaupel P, Schmidberger H, Mayer A. The Warburg effect: essential part of metabolic reprogramming and central contributor to cancer progression. Int J Radiat Biol. 2019;95(7):912–9.
24. Schwartz L, Supuran CT, Alfarouk KO. The Warburg effect and the hallmarks of cancer. Anticancer Agents Med Chem. 2017;17(2):164–70.
25. Shvedunova M, Akhtar A. Modulation of cellular processes by histone and non-histone protein acetylation. Nat Rev Mol Cell Biol. 2022;23(5):329–49.
26. Downey M. Non-histone protein acetylation by the evolutionarily conserved GCN5 and PCAF acetyltransferases. Biochim Biophys Acta Gene Regul Mech. 2021;1864(2):194608.
27. Moreno-Sanchez R, Saavedra E, Rodriguez-Enriquez S, Gallardo-Perez JC, Quezada H, Westerhoff HV. Metabolic control analysis indicates a change of strategy in the treatment of cancer. Mitochondrion. 2010;10(6):626–39.
28. Moreno-Sanchez R, Saavedra E, Rodriguez-Enriquez S, Olin-Sandoval V. Metabolic control analysis: a tool for designing strategies to manipulate metabolic pathways. J Biomed Biotechnol. 2008;2008:597913.
29. Fu Q, Yu Z. Phosphoglycerate kinase 1 (PGK1) in cancer: A promising target for diagnosis and therapy. Life Sci. 2020;256:117863.
30. Vander Heiden MG, Cantley LC, Thompson CB. Understanding the Warburg effect: the metabolic requirements of cell proliferation. Science. 2009;324(5930):1029–33.
31. Lv L, Xu YP, Zhao D, Li FL, Wang W, Sasaki N, Jiang Y, Zhou X, Li TT, Guan KL, et al. Mitogenic and oncogenic stimulation of K433 acetylation promotes PKM2 protein kinase activity and nuclear localization. Mol Cell. 2013;52(3):340–52.
32. Gao F, Zhang X, Wang S, Zheng L, Sun Y, Wang G, Song Z, Bao Y. TSP50 promotes the Warburg effect and hepatocyte proliferation via regulating PKM2 acetylation. Cell Death Dis. 2021;12(6):517.
33. Park SH, Ozden O, Liu G, Song HY, Zhu Y, Yan Y, Zou X, Kang HJ, Jiang H, Principe DR, et al. SIRT2-Mediated deacetylation and tetramerization of pyruvate kinase directs glycolysis and tumor growth. Can Res. 2016;76(13):3802–12.
34. Kim SC, Sprung R, Chen Y, Xu Y, Ball H, Pei J, Cheng T, Kho Y, Xiao H, Xiao L, et al. Substrate and functional diversity of lysine acetylation revealed by a proteomics survey. Mol Cell. 2006;23(4):607–18.
35. Horton JL, Martin OJ, Lai L, Riley NM, Richards AL, Vega RB, Leone TC, Pagliarini DJ, Muoio DM, Bedi KC, et al. Mitochondrial protein hyperacetylation in the failing heart. JCI Insight. 2016;2(1):e84897.
36. Yang H, Zhou L, Shi Q, Zhao Y, Lin H, Zhang M, Zhao S, Yang Y, Ling ZQ, Guan KL, et al. SIRT3-dependent GOT2 acetylation status affects the malate-aspartate NADH shuttle activity and pancreatic tumor growth. EMBO J. 2015;34(8):1110–25.
37. Wang M, Zhou C, Yu L, Kong D, Ma W, Lv B, Wang Y, Wu W, Zhou M, Cui G. Upregulation of MDH1 acetylation by HDAC6 inhibition protects against oxidative stress-derived neuronal apoptosis following intracerebral hemorrhage. Cell Mol Life Sci. 2022;79(7):356.
38. Domenech E, Maestre C, Esteban-Martinez L, Partida D, Pascual R, Fernandez-Miranda G, Seco E, Campos-Olivas R, Perez M, Megias D, et al. AMPK and PFKFB3 mediate glycolysis and survival in response to mitophagy during mitotic arrest. Nat Cell Biol. 2015;17(10):1304–16.
39. Li FL, Liu JP, Bao RX, Yan G, Feng X, Xu YP, Sun YP, Yan W, Ling ZQ, Xiong Y, et al. Acetylation accumulates PFKFB3 in cytoplasm to promote glycolysis and protects cells from cisplatin-induced apoptosis. Nat Commun. 2018;9(1):508.
40. Li J, Li S, Guo J, Li Q, Long J, Ma C, Ding Y, Yan C, Li L, Wu Z, et al. Natural Product Micheliolide (MCL) irreversibly activates pyruvate kinase M2 and suppresses leukemia. J Med Chem. 2018;61(9):4155–64.
41. Zheng S, Liu Q, Liu T, Lu X. Posttranslational modification of pyruvate kinase type M2 (PKM2): novel regulation of its biological roles to be further discovered. J Physiol Biochem. 2021;77(3):355–63.
42. Zhao S, Xu W, Jiang W, Yu W, Lin Y, Zhang T, Yao J, Zhou L, Zeng Y, Li H, et al. Regulation of cellular metabolism by protein lysine acetylation. Science. 2010;327(5968):1000–4.
43. Alleyn M, Breitzig M, Lockey R, Kolliputi N. The dawn of succinylation: a posttranslational modification. Am J Physiol Cell Physiol. 2018;314(2):C228–32.
44. Qi H, Ning X, Yu C, Ji X, Jin Y, McNutt MA, Yin Y. Succinylation-dependent mitochondrial translocation of PKM2 promotes cell survival in response to nutritional stress. Cell Death Dis. 2019;10(3):170.

45. Tong Y, Guo D, Lin SH, Liang J, Yang D, Ma C, Shao F, Li M, Yu Q, Jiang Y, et al. SUCLA2-coupled regulation of GLS succinylation and activity counteracts oxidative stress in tumor cells. Mol Cell. 2021;81(11):2303-2316 e2308.
46. Wang Y, Guo YR, Liu K, Yin Z, Liu R, Xia Y, Tan L, Yang P, Lee JH, Li XJ, et al. KAT2A coupled with the alpha-KGDH complex acts as a histone H3 succinyltransferase. Nature. 2017;552(7684):273–7.
47. Park J, Chen Y, Tishkoff DX, Peng C, Tan M, Dai L, Xie Z, Zhang Y, Zwaans BM, Skinner ME, et al. SIRT5-mediated lysine desuccinylation impacts diverse metabolic pathways. Mol Cell. 2013;50(6):919–30.
48. Ma Y, Qi Y, Wang L, Zheng Z, Zhang Y, Zheng J. SIRT5-mediated SDHA desuccinylation promotes clear cell renal cell carcinoma tumorigenesis. Free Radical Biol Med. 2019;134:458–67.
49. Du J, Zhou Y, Su X, Yu JJ, Khan S, Jiang H, Kim J, Woo J, Kim JH, Choi BH, et al. Sirt5 is a NAD-dependent protein lysine demalonylase and desuccinylase. Science. 2011;334(6057):806–9.
50. Yu HB, Cheng ST, Ren F, Chen Y, Shi XF, Wong VKW, Law BYK, Ren JH, Zhong S, Chen WX, et al. SIRT7 restricts HBV transcription and replication through catalyzing desuccinylation of histone H3 associated with cccDNA minichromosome. Clin Sci (Lond). 2021;135(12):1505–22.
51. Li L, Shi L, Yang S, Yan R, Zhang D, Yang J, He L, Li W, Yi X, Sun L, et al. SIRT7 is a histone desuccinylase that functionally links to chromatin compaction and genome stability. Nat Commun. 2016;7:12235.

Publisher's Note